Available online at www.sciencedirect.com
SCIENCE DIRECT
Spectrochimica Acta Part A 63 (2006) 383–390
SPECTROCHIMICA ACTA PART A
www.elsevier.com/locate/saa

# An ab initio study of the $C_2H_2$–HF, $C_2H(CH_3)$–HF and $C_2(CH_3)_2$–HF hydrogen-bonded complexes

Mozart N. Ramos [a,*], Kelson C. Lopes [b], Washington L.V. Silva [b], Alessandra M. Tavares [b], Fátima A. Castriani [b], Silmar A. do Monte [b], Elizete Ventura [b], Regiane C.M.U. Araújo [b]

[a] *Departamento de Química Fundamental, Universidade Federal de Pernambuco (UFPE), Rua Jose Simoes Araujo 352 apto 501, 50739-901, Recife (PE), Brasil*
[b] *Departamento de Química, Universidade Federal da Paraíba (UFPB), 58036-300, João Pessoa (PB), Brasil*

Received 24 February 2005; received in revised form 27 April 2005; accepted 14 May 2005

**Abstract**

MP2/6-31++G** and B3LYP/6-31++G** ab initio molecular orbital calculations have been performed in order to obtain molecular geometries, binding energies and vibrational properties of the $C_2H_2$–HF, $C_2H(CH_3)$–HF and $C_2(CH_3)_2$–HF H-bonded complexes. As expected, the more pronounced effects on the structural properties of the isolated molecules due to complexation was verified for the C≡C and H–F bond lengths, which are directly involved in the H-bond formation. These bond distances increased after complexation. BSSE uncorrected B3LYP binding energies are always lower than the corresponding MP2 values. However, the opposite trend has been verified after BSSE correction by the counterpoise method since it is much lower at B3LYP than at MP2 level. The binding energies for these complexes as well as for the HF acid submolecule modes (the HF stretching and vibrational frequency modes) showed an increasing hydrogen-bonding strength with increasing methyl substitution. The splitting in the HF in-plane and out-of-plane bending modes reflects the anisotropy in the hydrogen-bonding interaction with the π system of the C≡C bond. The H–F stretching frequency is shifted downward after complexation and it increases with the methyl substitution. The IR intensities of the HF acid submolecule fundamentals are adequately interpreted through the atomic polar tensor of the hydrogen atom using the charge–charge flux-overlap model. The skeletal stretching modes of the Alkyne submolecule are decreased in the complex. The new vibrational modes arising from complexation show several interesting features.


*Keywords:* Hydrogen bond; Ab initio methods; Infrared spectrum; Substituted alkyne

## 1. Introduction

A variety of experimental techniques and theoretical calculations has been employed in order to understand the hydrogen-bonding interaction with π-bonded systems. From the experimental point of view, the ground vibrational molecular structures of weakly hydrogen-bonded complexes have been characterized by means of microwave and infrared molecular beam techniques with a Fourier transform [1–7]. Nowadays, it is already well established that the molecular interaction between hydrogen halides as proton donors and alkynes or alkenes as proton acceptors produces T-type hydrogen complexes, which are T-shaped near-prolate asymmetric rotors. These complexes yield to X–H···π type interactions, i.e., the interaction between the hydrogen halide molecule HX and the π-electron density of a carbon–carbon triple or double bond. For example, Andrews et al. [7] have performed high-resolution FT-IR matrix isolation studies to identify a hydrogen-bonded π complex for $C_2H_2$–HX with $C_{2v}$ symmetry through comparison of the relatively small shifts for the C≡C stretching frequencies and relatively larger shifts for in-plane fundamental bending frequencies in the acetylene moieties and it was obtained a loss of degeneracy in all observed bending modes. On the other hand, theoretical calculations [8–13] have been particularly useful to estimate binding energies, H-bond lengths

* Corresponding author. Tel.: +55832167438; fax: +55832167437.
*E-mail address:* mozartnr@educacao.pe.gov.br (M.N. Ramos).

1386-1425/$ – see front matter © 2005 Elsevier B.V. All rights reserved.
doi:10.1016/j.saa.2005.05.024

and structural (electrical and vibrational) changes that take place in the isolated molecules after complexation. Moreover, theoretical calculations have been successful in predicting the new low-frequency vibrational modes, which, in general, show very weak intensities and, therefore, are difficult to characterize experimentally. These modes show several interesting features. However, high-level quantum chemical calculations with electron correlation and large basis set are necessary in order to obtain a proper description of a weakly bound hydrogen-bonded system. Generally, electron correlation effects are crucial to take into account dispersion forces. This can be reached through both Møller–Plesset perturbation theory at second-term level (MP2) [14] and density functional theory (DFT) [15] with B3LYP exchange-correlation functional. Furthermore, it is now well established that diffuse and polarization functions must be included in the basis set in order to adequately describe the non-spherical atomic densities and polarizability effects. This is particularly important in studying long-range electrostatic interactions.

The goal of the present paper is to study hydrogen-bonded complexes of the X–H $\cdots$ $\pi$ type, with hydrogen fluoride (HF) as proton donor, and acetylene ($C_2H_2$), methylacetylene [$C_2H(CH_3)$] and dimethylacetylene [$C_2(CH_3)_2$] as $\pi$-charge centre. The $C_2H_2$–HF, $C_2H(CH_3)$–HF and $C_2(CH_3)_2$–HF H-bonded complexes have been previously investigated by Andrews et al. [6] using Fourier transform infrared spectra, including also complexes of the type $C_2X_2$–HF with X = F and Cl [7]. They have shown that methyl substitution gives a stronger hydrogen bond and that halogen substitution gives a weaker hydrogen bond in a $\sigma$ complex involving the halogen. Their investigations consider the vibrational mode of the HF submolecule, leading to the conclusion that the more methyl groups replace hydrogen atoms the stronger the hydrogen bond becomes.

In this paper, a comparative investigation in terms of structural, electronic and vibrational properties of the $C_2H_2$–HF, $C_2H(CH_3)$–HF and $C_2(CH_3)_2$–HF H-bonded complexes have been performed at MP2 and B3LYP levels, with the 6-31++G** basis set.

## 2. Calculations

MP2/6-31++G** and B3LYP/6-31++G** ab initio calculations were performed by using the Gaussian 98W program [16]. In this procedure, the molecular geometries of the isolated compounds as well as the hydrogen-bonded complexes were fully optimized. The binding energies were computed considering the basis set superposition error (BSSE) [17] due to the super molecule approach using the full counterpoise (CP) method proposed by Boys and Bernardi [18]. It is important to point out that the procedure to estimate the BSSE correction including the fragment deformation energy in the estimation of BSSE correction to binding energy, as first highlighted by Ensley et al. [19] and stressed elsewhere [20,21] is, in general, minimized when the CP method is employed in conjunction with a large basis set, which is flexible enough to provide a good description of the electrons in both the atomic core and the long-range region of the atoms [22,23].

## 3. Results and discussion

The molecular geometries parameters of the $C_2H_2$–HF, $C_2H(CH_3)$–HF and $C_2(CH_3)_2$–HF complexes and of their isolated molecules were fully optimized at the MP2/6-31++G** and B3LYP/6-31++G** calculation levels. The results are shown in Fig. 1. As expected, the more pronounced effects verified after complexation were obtained for C≡C and H–F bond lengths, which are directly involved in the H-bond formation. Their increments ($\delta r_{C\equiv C}$ and $\delta r_{H-F}$) are given in Table 1 as well as the H-bond lengths measured from the fluorine atom of the H–F bond to the midpoint of the C≡C bond of the $C_2H_2$–HF and $C_2(CH_3)_2$–HF complexes. For the $C_2H(CH_3)$–HF complex, the H-bond distance is slightly closer to the carbon atom (of the triple bond) bonded to the hydrogen atom, so that the electronic repulsion between the methyl group and the hydrogen atom in HF is minimized. From Table 1, we can note that the C≡C and H–F bond distances increments after complexation increase with methyl substitution. For example, B3LYP values concerning the increment of H–F bond distances ($\delta r_{H-F}$) for the $C_2H_2$–HF, $C_2H(CH_3)$–HF and $C_2(CH_3)_2$–HF complexes are 0.010 Å, 0.014 Å and 0.017 Å, respectively. Thus, methyl substitution leads to a progressive increase in the increment of H–F bond distance with complexation. Although of smaller magnitude, the same trend holds for C≡C bond distances, for which $\delta r_{C\equiv C}$ values are 0.001 Å, 0.002 Å and 0.003 Å for the $C_2H_2$–HF, $C_2H(CH_3)$–HF and $C_2(CH_3)_2$–HF complexes, respectively, at both B3LYP and MP2 levels. On the other hand, the F $\cdots$ ||| hydrogen bond length is reduced by 0.07 Å on substitution of one hydrogen atom by a methyl group, at both B3LYP and MP2 levels. A second replacement causes a further decrease by the same quantity at MP2 level and by about 0.06 Å at B3LYP level. Therefore, our calculations indicate that methyl substitution produces a stronger hydrogen bond, in agreement with the results obtained by Andrews and Johnson [6,7]. Moreover, it is interesting to note that the hydrogen bond lengths obtained from MP2 results are always longer than the corresponding B3LYP values. For example, the MP2 value for $r_{F\cdots|||}$ is 3.107 Å in $C_2H_2$–HF, whereas its corresponding B3LYP value is 3.081 Å.

Table 2 shows the binding energies, $\Delta E$, the binding energies including zero point energy and BSSE correction, $\Delta E_c$, dipole moments ($\mu$) and polarity enhancements ($\Delta\mu$) for the $C_2H_2$–HF, $C_2H(CH_3)$–HF and $C_2(CH_3)_2$–HF complexes. $\Delta\mu$ stands for the dipole moment difference between the complex and the free molecules ($\Delta\mu = \mu_{complex} - \Sigma\mu_{free\ molecules}$). $\Delta E$ was determined by subtracting the sum of the total energies of the isolated molecules from the total energy of the hydrogen complex. Initially, we can note that the uncorrected binding energies,

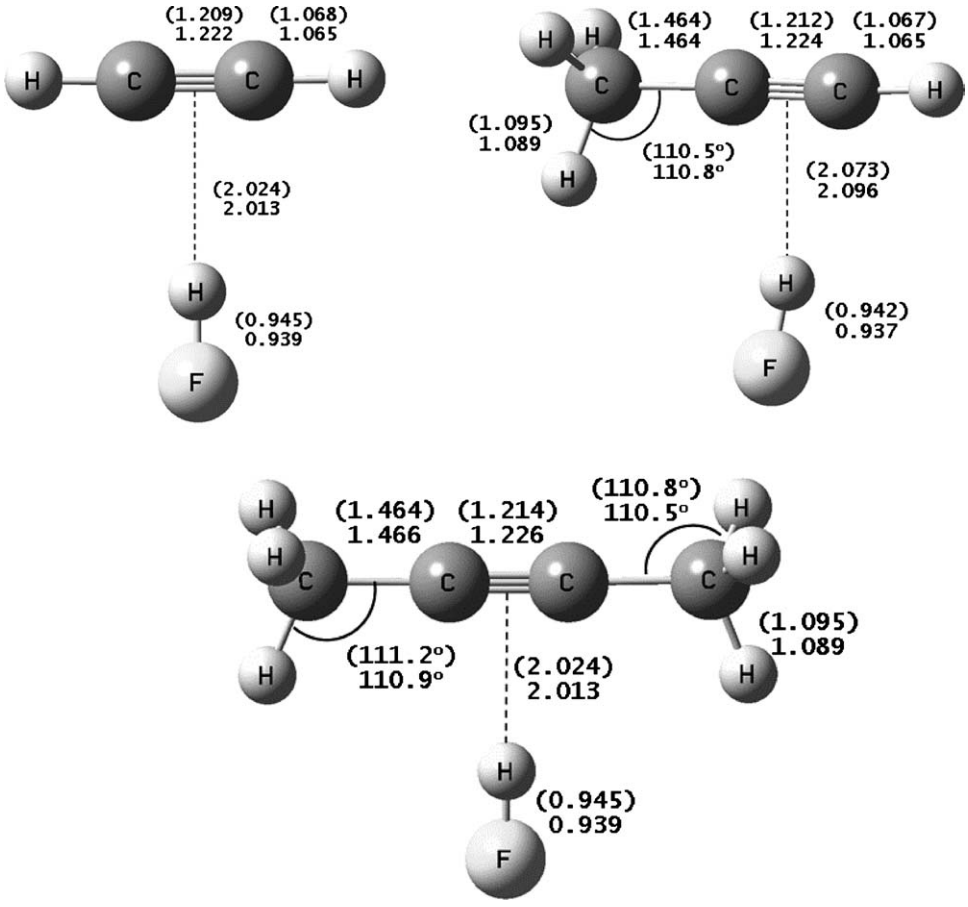


Fig. 1. MP2/6-31++G** and B3LYP/6-31++G** results for the full optimized geometries of $C_2H_2$—HF, $C_2H(CH_3)$—HF and $C_2(CH_3)_2$—HF H-bonded complexes. B3LYP values are given in parentheses. Units in angströms (Å).

Table 1
MP2/6-31++G** and B3LYP/6-31++G** values of the more pronounced structural changes occurring after complexation and the H-bond lengths

| Complexes | Level of calculation | Structural changes | | H-bond lengths $r_{F\ldots\vert\vert\vert}$ |
|---|---|---|---|---|
| | | $\delta r_{H-F}$ | $\delta r_{C\equiv C}$ | |
| $C_2H_2$—HF | MP2/6-31++G** | 0.007 | 0.001 | 3.107 |
| | B3LYP/6-31++G** | 0.010 | 0.001 | 3.081 (3.075)[a] |
| $C_2H(CH_3)$—HF | MP2/6-31++G** | 0.010 | 0.002 | 3.033 |
| | B3LYP/6-31++G** | 0.014 | 0.002 | 3.015 |
| $C_2(CH_3)_2$—HF | MP2/6-31++G** | 0.013 | 0.003 | 2.963 |
| | B3LYP/6-31++G** | 0.017 | 0.003 | 2.958 |

Units in angströms (Å).
[a] Refs. [6,7].

Table 2
MP2/6-31++G** and B3LYP/6-31++G** values of the hydrogen bonding energies, $\Delta E$ (defined as $\Delta E = E_A + E_B - E_{AB}$), BSSE, and corrected hydrogen bonding energies, $\Delta E_c$, which correspond to the binding energy after BSSE and zero point vibration energy correction

| Complexes | Level of calculation | $\Delta E$ | BSSE | $\Delta E_c$ | $(\mu)$ | $(\Delta\mu)$ |
|---|---|---|---|---|---|---|
| $C_2H_2$—HF | MP2/6-31++G** | 19.23 | 4.39 | 8.61 | 2.73 | 0.64 |
| | B3LYP/6-31++G** | 18.60 | 0.59 | 12.00 | 2.75 | 0.76 |
| $C_2H(CH_3)$—HF | MP2/6-31++G** | 24.75 | 4.76 | 12.96 | 2.83 | 0.74 |
| | B3LYP/6-31++G** | 23.53 | 0.38 | 16.97 | 2.97 | 0.98 |
| $C_2(CH_3)_2$—HF | MP2/6-31++G** | 28.97 | 5.10 | 16.89 | 2.89 | 0.79 |
| | B3LYP/6-31++G** | 26.75 | 0.21 | 20.23 | 2.93 | 0.94 |

Values in kJ mol$^{-1}$. Dipole moments and polarity enhancements ($\Delta\mu = \mu_{complex} - \Sigma\mu_{free\ molecules}$) in Debye.

$\Delta E$, obtained from the B3LYP results are always slightly lower than the corresponding MP2 values. However, a reverse trend is verified after BSSE correction is applied to the binding energy. Now, B3LYP values become larger than the MP2 values. Corrected B3LYP binding energies ($\Delta E_c$) are higher than the MP2 values by about of 4.0 kJ mol$^{-1}$. Chandra and Nguyen [13] have also verified the same behavior for the $C_2HX$–HX (X = F and Cl) complexes. As expected, our results indicate that lower H-bond lengths are associated with larger binding energies. In this same sense, our results also indicate an increasing hydrogen-bond strength with increasing methyl substitution: $\Delta E_c$ ($C_2(CH_3)_2$–HF) > $\Delta E_c$($C_2H(CH_3)$–HF) > $\Delta E_c$($C_2H_2$–HF) at both MP2 and B3LYP levels. Moreover, each methyl group leads to an increase of about ∼4.0 kJ mol$^{-1}$ in $\Delta E_c$. It is interesting to point out that the values of $\Delta E_c$ for $C_2HF$–HF obtained by Chandra and Nguyen [13] employing the MP2/6-31++G** and B3LYP/6-31++G** calculations are 3.51 and 7.48 kJ mol$^{-1}$, respectively. These results confirm that methyl substitution gives a stronger hydrogen bond and that halogen substitution gives a weaker hydrogen bond.

Large polarity enhancements due to complexation are found for the $C_2H_2$–HF, $C_2H(CH_3)$–HF and $C_2(CH_3)_2$–HF complexes; the values are in the range of 0.6–0.8 D at MP2 level, and 0.8–1.0 D at B3LYP level. These polarity enhancements tend to increase with the methyl substitution in the $C_2X_2$ base molecule.

The vibrational spectrum of a hydrogen-bonded complex contains bands due to acid (HF) and base ($C_2X_2$) submolecules which differ from the free acid and base molecules depending on the strength and orientation of the hydrogen-bonding interaction. For the above complexes, Andrews et al. [1,2,6,7] have already observed that the strongest acid submolecule modes are the H–F stretching fundamental ($\nu_{HF}^{str}$) and the H–F deformation fundamentals ($\nu_{\beta,\text{ in-plane}}$ and $\nu_{\beta,\text{ out-of-plane}}$), which are split due to an anisotropy of the HF interaction with the π-charge centre. They have also observed that the base submolecule modes are only slightly shifted by the HF ligand and, therefore, the base molecule may be useful as a model for the base submolecule in the complex. From the theoretical point of view, Chandra and Nguyen [13] confirm the experimental observations from Andrews and collaborators for the $C_2HX$–HX complexes with X = F and Cl. They have also verified that the H–X stretching frequency shift and the intermolecular vibrational frequencies are better estimated at B3LYP than at MP2 level, using the 6-31++G** basis set. However, IR intensities have not been considered in both experimental and theoretical studies. Thus, we have listed in Table 3 the MP2/6-31++G** and B3LYP/6-31++G** results of the harmonic frequencies, frequency shifts, infrared intensities and intensity ratios after complexation for the HF stretching mode in $C_2H_2$–HF, $C_2H(CH_3)$–HF and $C_2(CH_3)_2$–HF complexes. The previous experimental values obtained from Andrews and Johnson [6,7] and the theoretical values for $C_2HF$–HF obtained from Chandra and Nguyen [13] are given in Table 3. From this table, we can verify that the H–F stretching frequency is shifted downward after complexation. Moreover, we can still notice that larger shifts are associated with stronger hydrogen bonds in considering values of $\Delta E_c$ shown in Table 2. In Fig. 2 the values of $\Delta E_c$ against the experimental stretching frequency shifts are given. The greater shift ($\Delta\nu_{HF}^{str}$) is found for the $C_2(CH_3)_2$–HF system, which corresponds to the more strongly bound complex, whereas the lower shift is found for the $C_2HF$–HF complex that represents the more weakly bound complex. From Table 3 we can also note that the $\Delta\nu_{HF}^{str}$ experimental values are situated between those obtained from MP2 and B3LYP methods. However, they are slightly nearest to the B3LYP ones.

From Table 3 one can see that the H–F stretching intensity of the proton donor molecule is much enhanced upon H-bond formation. For example, the $A_{HF}^{str,C}/A_{HF}^{str}$ ratio in $C_2(CH_3)_2$–HF is 6.1 and 8.0 at MP2 and B3LYP levels, respectively. The intensity ratios obtained from B3LYP are always higher than the MP2 ones. Unfortunately, as far as we are concerned, the experimental value for the H–F stretching intensity after complexation is unknown. Thus, this prevents

Table 3
MP2/6-31++G** and B3LYP/6-31++G** values of the harmonic frequencies, frequency shifts, infrared intensities and intensity ratios after complexation of the HF stretching

| Compounds | Level of calculation | $\nu_{HF}^{str}$ | $\nu_{HF}^{str,C} - \nu_{HF}^{str}$ | $A_{HF}^{str}$ | $A_{HF}^{str,C}/A_{HF}^{str}$ |
|---|---|---|---|---|---|
| HF | MP2/6-31++G** | 4119 | – | 126 | – |
| | B3LYP/6-31++G** | 4068 (3961)[a] | – | 114 (77)[b] | – |
| $C_2H_2$–HF | MP2/6-31++G** | – | 161 | – | 4.7 |
| | B3LYP/6-31++G** | – | 241 (208.3)[a] | – | 6.3 |
| $C_2H(CH_3)$–HF | MP2/6-31++G** | – | 233 | – | 5.2 |
| | B3LYP/6-31++G** | – | 326 (280.4)[a] | – | 7.2 |
| $C_2(CH_3)_2$–HF | MP2/6-31++G** | – | 308 | – | 6.1 |
| | B3LYP/6-31++G** | – | 402 (354.9)[a] | – | 8.0 |
| $C_2HF$–HF[c] | MP2/6-31++G** | – | 133 | | |
| | B3LYP/6-31++G** | – | 214 (184) | | |

Experimental values are given in parentheses. Units in cm$^{-1}$ and km mol$^{-1}$.
[a] Ref. [6].
[b] Ref. [7].
[c] Ref. [13].

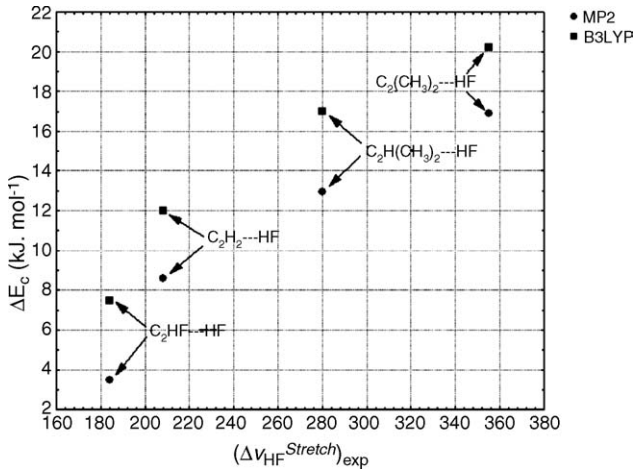


Fig. 2. Values of $\Delta E_c$ against the H–F experimental stretching frequency shifts in the $C_2H_2$–HF, $C_2H_2$–HF, $C_2H(CH_3)$–HF and $C_2(CH_3)_2$–HF series.

a direct comparison between calculated and experimental intensity ratios. Nowadays, on the other hand, it is well known that this increase in the H–X (X = F, Cl, CN, NC and CCH) stretching intensity is due to the charge-flux term [9,10,12], which is strongly affected by complexation, in contrast to what happens with the hydrogen charge. The latter is always positive whereas the charge-flux is slightly negative in the free molecule and becomes quite positive after complexation. In the complex, the hydrogen charge and the charge-flux term have the same algebraic sign; then, since the HX stretching intensity is proportional to the sum of the squares of these terms, it is enormously increased upon H-bond formation. The modified charge–charge flux-overlap (CCFO) model [24,25] for infrared intensities has shown the importance of the charge-flux term in the H–X stretching intensity enhancement. Here, we can confirm this behavior through comparison between $P^{H}_{xx}$ and $P^{H}_{zz}$ elements of the atomic polar tensor for the hydrogen atom before and after complexation. According with the modified CCFO model, the $P^{H}_{xx}$ element is a measure of the hydrogen atomic charge at equilibrium position whereas the $P^{H}_{zz}$ element measures the sum of the hydrogen atomic charge ($P^{H}_{xx}$) and the charge-flux term associated to the H–F stretching. Table 4 gives the results of the atomic polar tensor for the hydrogen atom ($P^{H}_{X}$) before and after complexation with $C_2H_2$, $C_2H(CH_3)$ and $C_2(CH_3)_2$. For example, the $P^{H}_{xx}$ element in free HF is 0.451e and after complexation with $C_2H_2$ its value is decreased to 0.359e. On the other hand, the $P^{H}_{zz}$ element is 0.352e in free HF and becomes 0.765e after complexation, i.e., it is more than twice the $P^{H}_{xx}$ element in the complex. The modified CCFO model shows that the $P^{H}_{zz}$ element can be represented by:

$$P^{H}_{zz} = q^{o}_{H} + (\partial q_H/\partial z_H) r^{o}_{H} \quad (1)$$

whereas the $P^{H}_{xx}$ element is given by:

$$P^{H}_{xx} = q^{o}_{H} \quad (2)$$

Table 4
MP2/6-31++G** and B3LYP/6-31++G** values of the atomic polar tensor of the hydrogen atom in free and after complexation with HF

| Compounds | $P^{H}_{x} =$ |
|---|---|
| | $\begin{bmatrix} P^{H}_{xx} & & \\ & P^{H}_{yy} & \\ & & P^{H}_{zz} \end{bmatrix}$ |
| y ↑ H–F → z | $\begin{pmatrix} 0.451(0.447) & & \\ & 0.451(0.447) & \\ & & 0.352(0.334) \end{pmatrix}$ |
| $C_2H_2$–HF | $\begin{pmatrix} 0.359(0.340) & & \\ & 0.294(0.272) & \\ & & 0.765(0.849) \end{pmatrix}$ |
| $C_2H(CH_3)$–HF | $\begin{pmatrix} 0.334(0.316) & & \\ & 0.268(0.239) & \\ & & 0.822(0.913) \end{pmatrix}$ |
| $C_2(CH_3)_2$–HF | $\begin{pmatrix} 0.312(0.296) & & \\ & 0.250(0.221) & \\ & & 0.876(0.954) \end{pmatrix}$ |

Units of electrons, *e*. B3LYP values are given in parentheses.

Moreover, the H–X stretching intensity can be represented by:

$$A^{str}_{HF} = K(P^{H}_{zz})^2 \quad (3)$$

where K = 975 km mol$^{-1}$ e$^{-2}$ for values of IR intensities in km mol$^{-1}$. These three equations allow us to get a better understanding of why the H–F stretching intensity is much enhanced after complexation, specially the effect of the charge-flux term ($\partial q_H/\partial z_H$) on its value. For the H-bonded complexes systems investigated in this work, the charge-flux term changes from 0.334e in free HF to 0.849e in $C_2H_2$–HF, to 0.913e in $C_2H(CH_3)$–HF and finally, to 0.954e in $C_2(CH_3)_2$–HF complex at B3LYP level. Similar behavior was obtained at MP2 level. It is also interesting to verify that the charge-flux is negative in the free molecule ($P^{H}_{zz} < P^{H}_{xx}$, −0.113e for B3LYP and −0.099e for MP2 in HF) and becomes quite positive after complexation ($P^{H}_{zz} < P^{H}_{xx}$, +0.509e for B3LYP and +0.406e for MP2 in $C_2H_2$–HF). Other important observed feature is that the $P^{H}_{zz}$ element increases with the H-bond strength.

Using the Eq. (3) we can make a self-check of the calculated H–F stretching intensities. In free HF, the intensities obtained from this equation are 121 and 109 km mol$^{-1}$, using the MP2 and B3LYP results for $P^{H}_{zz}$, whereas the corresponding values obtained directly from a normal mode analysis are 126 and 114 km mol$^{-1}$, respectively. Concerning $C_2H(CH_3)$–HF complex, the values obtained from Eq. (3) together with the polar tensors obtained from MP2 and B3LYP calculations are 659 and 813 km mol$^{-1}$, respectively, whereas the corresponding values obtained from a normal mode analysis are 658 and 823 km mol$^{-1}$, respectively. The values coming from Eq. (3) are clearly in very good agreement with the obtained directly from a frequency calculation. This means that the normal mode for this vibration is dominated by the movement of the hydrogen atom along the axis of the H–F bond, which it is here represented by the

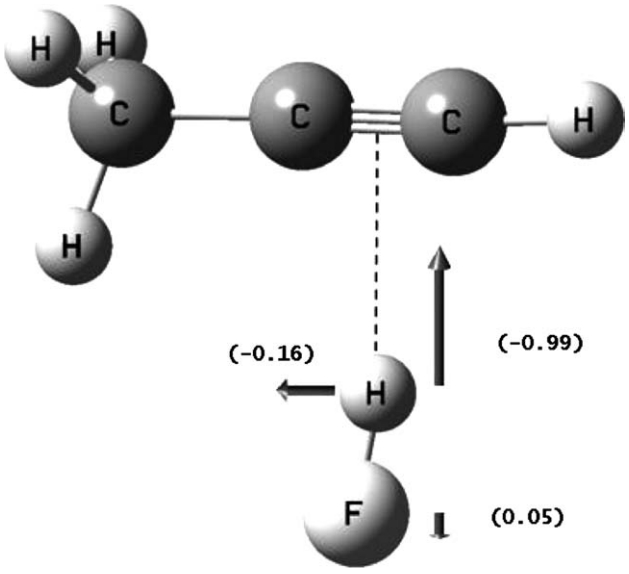


Fig. 3. Normal coordinate for the HF stretching mode using the B3LYP level of calculation.

$z$ Cartesian axis. In Fig. 3 we show the normal mode for the H–F stretching in $C_2H(CH_3)$–HF obtained from the B3LYP calculation. The relative lengths of the vectors representing the atomic displacements for this normal mode are given in parentheses. It is important to draw the attention to the fact that the hydrogen displacement (−0.16) perpendicular to the $z$-axis is due to molecular asymmetry of the π-charge centre in $C_2H(CH_3)$–HF. It does not appear in $C_2H_2$ and $C_2(CH3)_2$.

In contrast to what happens with the HF stretching mode after complexation, the stretching frequencies of the $C_2X_2$ moiety are only slightly modified by the HF acid. In Table 5 we can verify that the experimental and B3LYP values for $\Delta\nu_{C–H}$ are only $-9\,cm^{-1}$ and $-12\,cm^{-1}$, respectively. These same displacements are also verified to $\Delta\nu_{C\equiv C}$. Our results show that the alkyne submolecule stretching modes are decreased after complexation. It is still interesting to note that $\Delta\nu_{C\equiv C}$ increases upon methyl substitution: $-7\,cm^{-1}$ for $C_2H_2$–HF, $-12\,cm^{-1}$ for $C_2H(CH_3)$–HF and $-16\,cm^{-1}$ for $C_2(CH_3)_2$–HF, at B3LYP level. Their IR intensities are very weak in both free molecule and the complex. On the other hand, the C–H stretching intensity of the HCCX base molecule both before and after complexation are relatively large. For example, the C–H stretching intensity is $64\,km\,mol^{-1}$ in $C_2H(CH_3)$ and changes to $85\,km\,mol^{-1}$ after complexation. Therefore, its $A^{str,\,C}_{C–H}/A^{str}_{C–H}$ ratio is equal to 1.3.

The formation of the $C_2H_2$–HF, $C_2H(CH_3)$–HF and $C_2(CH_3)_2$–HF complexes gives rise to new vibrational modes, which the low-frequency ones are given in Table 6. Fig. 4 shows the schematic representation of these new normal modes in $C_2H_2$–HF obtained at B3LYP calculations. These new modes exhibit several interesting features. (i) Initially, we can verify that the H-stretch frequency follows the order: $C_2(CH_3)_2$–HF > $C_2H(CH_3)$–HF > $C_2H_2$–HF > $C_2H$F–HF, i.e., $204\,cm^{-1}$, $157\,cm^{-1}$, $139\,cm^{-1}$ and $135\,cm^{-1}$[13], respectively. Therefore, its value increases with increasing methyl substitution. Its IR intensity is, in turn, very weak and thus, it is not easy to be characterized from its experimental vibrational spectrum. (ii) The two H–F bending modes, which are associated with the in-plane ($b_2$) and out-of-plane ($b_1$) bending modes, where the proton of the HF molecule moves along a line which is perpendicular to the H–F chemical bond axis, have appreciable intensities. These modes, which are pure rotations in the HF isolated molecule, become infrared-active after complexation. The out-of-plane bending intensity is practically determined by the hydrogen equilibrium charge, i.e., the $P^H_{xx}$ element of the atomic polar tensor of the hydrogen atom in HF (Table 4). From Table 6 we can see that its B3LYP calculated values (from a frequency calculation) for the $C_2(CH_3)_2$–HF, $C_2H(CH_3)$–HF and $C_2H_2$–HF are 100.9, 76.3 and $95.9\,km\,mol^{-1}$, respectively, whereas the values obtained by using the equation:

$$A^{\text{out-of-plane}}_{HF} = K(P^H_{xx})^2 \quad (4)$$

are 113, 97 and $85\,km\,mol^{-1}$, respectively, which are in reasonable agreement with the calculated ones. The in-plane bending mode ($\nu_{\beta,\text{ in-plane}}$) has also appreciable intensity but its value is practically half of that relative to the out-of-plane mode. For example, this latter is $100.9\,km\,mol^{-1}$ in $C_2H_2$–HF whereas its corresponding value for the in-plane mode is $56.6\,km\,mol^{-1}$. Andrews and Johnson [6,7] have pointed out that this splitting reflects an anisotropic potential governing the liberation of HF against the π-charge centre of the $C_2X_2$ base sub molecule. They have also observed that the in-plane bending mode has the higher potential because of a small contribution from repulsion between the HF acid and acetylenic protons. This split tends to

Table 5
B3LYP/6-31++G** values of the C–H and C≡C stretching frequencies ($\nu_i$, $cm^{-1}$) and IR intensities ($A_i$, $km\,mol^{-1}$) for the $C_2H_2$ and $C_2H(CH_3)$ molecules before and after complexation with HF

| Assign | $C_2H_2$ | $C_2H_2$–HF | $\Delta\nu_i$ or $A_i{}^C/A_i{}^{is}$ | $C_2H(CH_3)$ | $C_2H(CH_3)$–HF | $\Delta\nu$ or $A_i{}^C/A_i{}^{is}$ |
|---|---|---|---|---|---|---|
| C–H stretch | | | | | | |
| $\nu_I$ | 3430 (3289) | 3419 (3281) | −11 (−8) | 3484 (3323) | 3472 (3312) | −12 (−9) |
| $A_i$ | 93 | 124 | 1.3 | 64 | 85 | 1.3 |
| C≡C stretch | | | | | | |
| $\nu_I$ | 2069 (1974) | 2062 (1973) | −7 (−1) | 2227 (2137) | 2215 (2128) | −12 (−9) |
| $A_i$ | 0 | 1 | | 9 | 14 | 1.6 |

Experimental values are given in parentheses.

Table 6
B3LYP/6-31++G** and experimental[a] values of intermolecular harmonic frequencies ($\nu_i$, $cm^{-1}$) and IR intensities ($A_i$, km $mol^{-1}$)

| New vibrational modes | $C_2H_2$—HF | | $C_2H(CH_3)$—HF | | $C_2(CH_3)_2$—HF | |
|---|---|---|---|---|---|---|
| | Exp | B3LYP | Exp | B3LYP | Exp | B3LYP |
| $H_{bond}$-stretch ($a_1$)[b] | | | | | | |
| $\nu_\sigma$ | 87 | 139 | – | 157 | – | 204 |
| $A_\sigma$ | – | 1.1 | – | 3.3 | – | 6.1 |
| H—F bend ($b_2$) | | | | | | |
| $\nu_{\beta,\ in\text{-}plane}$ | 426 | 499 | 490 | 558 | 552 | 656 |
| $A_{\beta,\ in\text{-}plane}$ | – | 56.6 | – | 43.4 | – | 51.5 |
| H—F bend ($b_1$) | | | | | | |
| $\nu_{\beta,\ out\text{-}of\text{-}plane}$ | 382 | 437 | 432 | 489 | 489 | 530 |
| $A_{\beta,\ out\text{-}of\text{-}plane}$ | – | 100.9 | – | 76.3 | – | 95.9 |
| H-bend ($b_2$) | | | | | | |
| $\nu_B$ | – | 96 | – | 61 | – | 57 |
| $A_B$ | – | 6.3 | – | 4.8 | – | 3.7 |

[a] Ref. [13].
[b] This mode consists of a combination between a HF stretching and an intermolecular mode (see Fig. 4(b) for details), which approximates the HF and alkyne molecules.

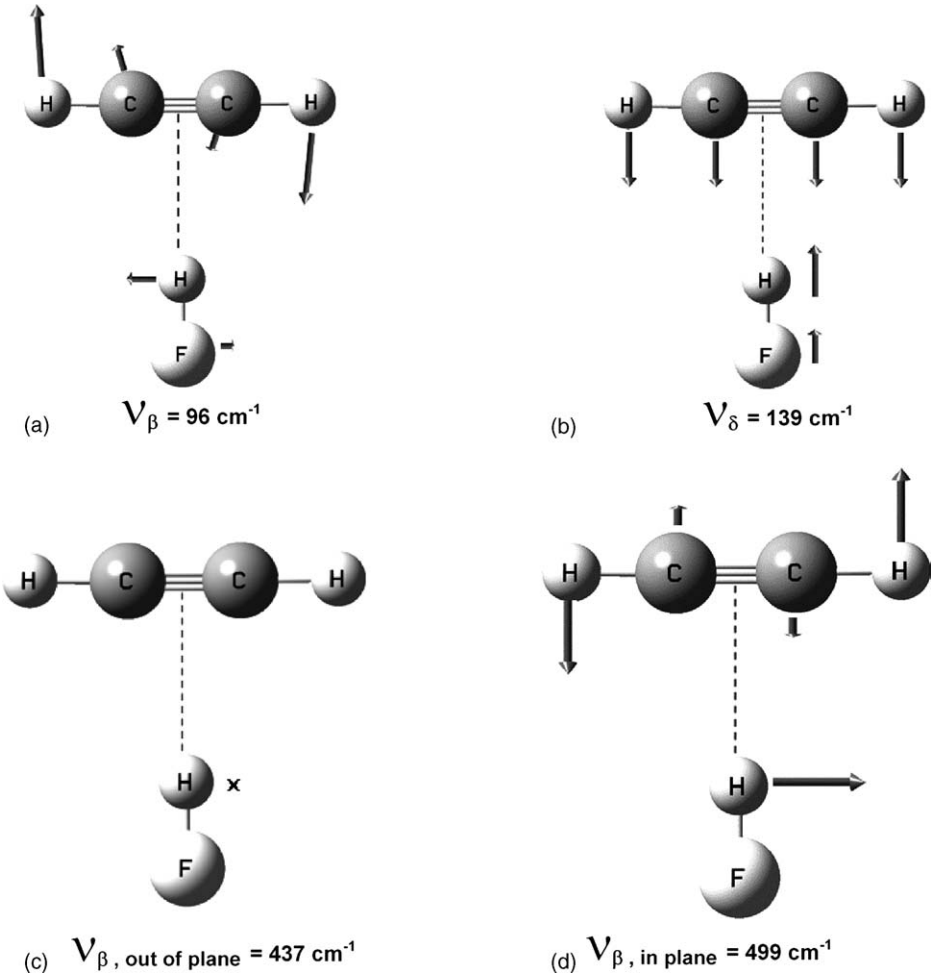


Fig. 4. New intermolecular vibrational modes obtained from the B3LYP/6-31++G** calculations for the $C_2H_2$—HF complex.

increase in the series: $C_2HF{-}HF$, $C_2H_2{-}HF$, $C_2H(CH_3){-}HF$ and $C_2(CH_3)_2{-}HF$. The experimental values [6,7] for $\Delta\nu_\beta$ ($\nu_{\beta,\text{ in-plane}} - \nu_{\beta,\text{ out-of-plane}}$) are $30\,cm^{-1}$, $44\,cm^{-1}$, $58\,cm^{-1}$ and $63\,cm^{-1}$, respectively. (iii) The lowest-frequency mode of each complex consists of an intermolecular bending vibration, where the atoms in each molecule in the complex move in a direction perpendicular to the respective molecular axis, as shown schematically in Fig. 4(a). Its IR intensity is very weak and tends to decrease with the methyl substitution, as well as its vibrational frequency. For example, its B3LYP values for the $C_2H_2{-}HF$, $C_2H(CH_3){-}HF$ and $C_2(CH_3)_2{-}HF$ complexes are $96\,cm^{-1}$, $61\,cm^{-1}$ and $57\,cm^{-1}$, respectively.

## 4. Conclusions

Our MP2/6-31++G** and B3LYP/6-31++G** calculations have confirmed the previous vibrational spectroscopic evidences obtained by Andrews and Johnson [6,7], that is, the H-bond strength increases in the $C_2H_2{-}HF$, $C_2H(CH_3){-}HF$ and $C_2(CH_3)_2{-}HF$ series. Their binding energies with or without zero-point energy and BSSE correction clearly indicate this behavior, i.e., an increasing H-bond strength with increasing methyl substitution. This also produces a greater shift on the H–F stretching frequency after complexation and an increasing splitting in the H–F vibrational modes and the CCH deformation mode. The IR intensities of the HF acid sub molecule modes (the H–F stretching and vibrational fundamental frequencies) are adequately interpreted through the atomic polar tensor of the hydrogen atom in HF. Our calculations also show small red shifts of the base submolecule skeletal stretching modes.

## Acknowledgements

The authors gratefully acknowledge partial financial support from the Brazilian funding agencies CNPq, CAPES and FINEP.

## References

[1] S.A. McDonald, G.L. Johnson, B.W. Keelan, L. Andrews, J. Am. Chem. Soc. 102 (1980) 2892.
[2] L. Andrews, G.L. Johnson, B.J. Kelsall, J. Chem. Phys. 76 (1982) 5767.
[3] G.W. Bryant, D.F. Eggers, R.O. Watts, J. Chem. Soc. Faraday Trans. 284 (1988) 1443.
[4] A.C. Legon, P.D. Aldrich, W.H. Flygare, J. Chem. Phys. 75 (1981) 625.
[5] P.D. Aldrich, A.C. Legon, W.H. Flygare, J. Chem. Phys. 75 (1981) 2126.
[6] L. Andrews, G.L. Johnson, J. Phys. Chem. 86 (1982) 3380.
[7] L. Andrews, G.L. Johnson, J. Phys. Chem. 86 (1982) 3374.
[8] T.-H. Tang, W.-J. Hu, D.-Y. Yan, Y.-P. Cui, J. Mol. Struct. (Theochem) 207 (1990) 319.
[9] R.C.M.U. Araújo, J.B.P. da Silva, M.N. Ramos, Spectrochim. Acta 51A (1995) 821.
[10] K.C. Lopes, F.S. Pereira, M.N. Ramos, R.C.M.U. Araújo, Spectrochim. Acta 57A (2001) 1339.
[11] A.K. Chandra, P. Sourav, A.C. Limaye, S.R. Gadre, Chem. Phys. Lett. 247 (1995) 95.
[12] K.C. Lopes, F.S. Pereira, R.C.M.U. Araújo, M.N. Ramos, J. Mol. Struct. 565 (2001) 417.
[13] A.K. Chandra, M.T. Nguyen, Chem. Phys. 232 (1998) 299.
[14] C. Moller, M.S. Plesset, Phys. Rev. 46 (1934) 618.
[15] (a) A.D. Becke, J. Chem. Phys. 98 (1993) 5648;
(b) C. Lee, W. Yang, R.G. Parr, Phys. Rev. B 37 (1988) 785.
[16] Frisch M.J., Trucks G.W.; Head-Gordon M., Gill P.M.W., Wong M.W., Foresman J.B., Johnson B.G., Schlegel H.B., Robb M.A., Replogle E.S., Gomperts R., Andres J.L., Raghavachari K., Binkley J.S., Gonzales C., Martin R.L., Fox D.J., Defrees D.J., Baker J., Stewart J.J.P., Pople J.A., Gaussian 98W (Revision A11.2), Gaussian, Inc., Pittsburgh, PA, 2001.
[17] N.R. Kestner, J. Chem. Phys. 48 (1968) 252.
[18] S.F. Boys, F. Bernardi, Mol. Phys. 19 (1970) 553.
[19] J. Emsley, O.P.A. Hoyte, R.E. Overill, J. Am. Chem., Soc. 100 (1978) 3303.
[20] L. Turi, J.J. Dannenberg, J. Phys. Chem. 97 (1993) 2488.
[21] S.S. Xantheas, J. Chem. Phys. 104 (1996) 8821.
[22] D. Feller, J. Chem. Phys. 96 (1992) 6104.
[23] J.J. Novoa, M. Planas, M.-H. Whangbo, Chem. Phys. Lett. 225 (1994) 240.
[24] W.T. King, G.B. Mast, J. Phys. Chem. 80 (1976) 2521.
[25] M.N. Ramos, M. Gussoni, C. Castiglioni, G. Zerbi, Chem. Phys. Lett. 151 (1988) 397.